CrossMark

NOTE

Complementary analysis of curcumin biodistribution using optical fluorescence imaging and mass spectrometry

Yoon Young Kang[1] · Inseong Choi[2] · Youhoon Chong[2] · Woon-Seok Yeo[2] · Hyejung Mok[1]

Abstract In this study, a complementary analysis was performed to improve the precision of the determination of in vivo curcumin biodistribution after intravenous administration. Overall, similar curcumin biodistribution profiles were obtained using optical fluorescence imaging and mass spectrometry. Poor curcumin accumulation was observed in the heart, spleen, and kidney. However, noticeable accumulation of curcumin in the brain was only observed using fluorescence imaging, probably owing to the insufficient extraction of curcumin from the brain for mass spectrometry. In addition, an exact and reliable measurement of curcumin accumulation in tissues such as the liver, gallbladder, and pancreas was performed using mass spectrometry because of high autofluorescence. Taken together, complementary analysis using optical fluorescence imaging and mass spectrometry allowed the precise determination of curcumin in each tissue. Furthermore, this complementary analytical strategy could be used to elucidate the in vivo distribution of a wide range of fluorescent polyphenols.

Yoon Young Kang and Inseong Choi have been contributed equally to this study.

✉ Woon-Seok Yeo
  wsyeo@konkuk.ac.kr

✉ Hyejung Mok
  hjmok@konkuk.ac.kr

[1] Department of Bioscience and Biotechnology, Konkuk University, Seoul 05029, Republic of Korea

[2] Department of Bioscience and Biotechnology, Bio/Molecular Informatics Center, Konkuk University, Seoul 05029, Republic of Korea

Introduction

Curcumin is a natural hydrophobic polyphenol isolated from herbs such as the rhizome of turmeric (Anand et al. 2007; Naksuriya et al. 2014). Despite its diverse bioactivities and therapeutic safety, curcumin has shown limited applicability due to its poor solubility and fast elimination from the human body (Anand et al. 2007). Additionally, curcumin can be rapidly metabolized to ferulic acid, dihydroferulic acid, and other curcumin derivatives including curcumin glucuronide, which reduces its biological activities (Anand et al. 2007). Therefore, the in vivo fate of curcumin including its bioavailability and biodistribution has been vigorously examined using diverse analytic methods, e.g., high-performance liquid chromatography (HPLC) and mass spectrometry (MS) after tissue extraction (Kakkar et al. 2013; Pan et al. 1999; Tsai et al. 2011). In particular, the use of mass analysis has advantages over other analytical methods including low background signals, no false-positive signals, multiplexing capability, intrinsic label-free detections, and high sensitivity along with instrumental advances (Kim et al. 2015). However, these methods require extraction processes, which require optimization for different tissues and organs and therefore are often not reliable. In addition, considering the poor stability of curcumin at physiological pH, the analysis of curcumin without performing an extraction is also crucial to elucidating its fate in vivo. A previous study reported that more than 60 % of curcumin was degraded after incubation for 5 min at pH 7.2 (Pan et al. 1999). Alternatively, curcumin can be monitored directly by

optical fluorescence imaging to avoid extraction processes due to its fluorescent nature. Optical fluorescence imaging methods have numerous advantages for in vivo evaluation of biomolecules such as simplicity of use, rapid detection, and real-time monitoring of biomolecules without time-consuming extraction processes. However, several inherent challenges such as false positives due to autofluorescence, high signal-to-noise ratios, and low sensitivity remain (Choy et al. 2003). Therefore, complementary analytic strategies combining mass analysis and optical fluorescence imaging are required for the precise monitoring of curcumin processing in vivo. To the best of our knowledge, comparative experiments using two different analytic methods have not yet been reported in the elucidation of the in vivo distribution of curcumin quantitatively and qualitatively.

Therefore, in this study, the biodistribution of curcumin was comparatively analyzed by simultaneously combining optical fluorescence imaging and matrix-assisted laser desorption/ionization time-of-flight mass spectrometry (MALDI-TOF-MS). After intravenous injection of curcumin at a dose of 25 mg/kg, its location was visualized using fluorescence imaging without extraction. In addition, after curcumin was extracted from each organ, the amount was quantitatively analyzed using MS.

Materials and methods

Materials

Curcumin, dimethyl sulfoxide (DMSO), ethyl acetate (EA), α-cyano-4-hydroxycinnamic acid (CHCA), acetonitrile (ACN), sodium dodecyl sulfate (SDS), and kolliphor were purchased from Sigma-Aldrich (St. Louis, MO, USA). Dimethylated curcumin (internal standard) was prepared as described in a previous report (Kim et al. 2011). The phosphate-buffered saline (PBS) solution was obtained from Gibco BRL (Grand Island, NY, USA). ICR mice (six-week-old, female) were purchased from Orient Bio Inc. (Seong-nam, Korea). All other chemicals were of analytical grade.

Intravenous injection and optical fluorescence imaging of curcumin

ICR mice (n = 2–3) were anesthetized via intraperitoneal injection of Rompun/Zoletil according to the manufacturer's protocol (Zhang et al. 2015) and then injected intravenously with freshly prepared curcumin (25 mg/kg) in PBS containing 15 % (v/v) each of kolliphor and DMSO. The biodistribution of curcumin was monitored 1 h post administration. After the mice had been euthanized, their organs were collected and washed with PBS.

The samples were frozen and stored at −70 °C until analyzed. Fluorescence images of each organ were acquired using the In Vivo Imaging System (IVIS, Caliper Life Sciences Lumina II, Massachusetts, USA) at excitation and emission wavelengths of 430 and 509 nm, respectively. The total flux of the whole organs at the region of interest was also quantitatively analyzed with the IVIS using the following equation: total flux$_{injected}$ − total flux$_{control}$. All animal care and experimental procedures were approved by the Animal Care Committee of Konkuk University.

Construction of calibration curve

Curcumin at various concentrations ranging from 200 μM to 200 nM (10 μL in ACN) was mixed with 10 μM of dimethylated curcumin as an internal standard (10 μL in ACN). The resulting mixture was analyzed using MALDI-TOF MS with CHCA as a matrix.

Extraction

To quantify the curcumin contents of different tissues and organs including the brain, lung, liver, spleen, pancreas, kidney, and gall bladder, curcumin was extracted using EA. In brief, tissues were weighed and homogenized in PBS (pH 7.4, tissue:PBS = 1:3, w/v). Then, 500 μL samples of the homogenates were mixed with 200 and 500 μL of 10 % SDS and EA, respectively, followed by sonication for 10 min. The mixture was centrifuged at 6000 rpm for 2 min, the supernatant was collected and extracted thrice with equal volumes of EA, and then the combined organic layer was dried at room temperature.

Mass analysis

The dried tissue extracts were reconstituted with 20 μL of the internal standard solution (5 μM in ACN). Then, equal volumes (6 μL) of the sample and CHCA solutions were mixed, and 1.5 μL of the mixture was analyzed using MALDI-TOF MS. Mass analysis was performed with an Autoflex III MALDI-TOF mass spectrometer (Bruker Daltonics, Bremen, Germany) with a Smartbeam laser as the ionization source. All the spectra were acquired using an accelerating voltage of 19 kV and 50 Hz repetition rate in the positive mode with an average of 500 shots using CHCA (5 mg/mL in ACN) as the matrix.

Results and discussion

Figure 1 shows the schematic illustration of two different analytic strategies using in vivo optical imaging instrument and MS to determine the biodistribution of curcumin after
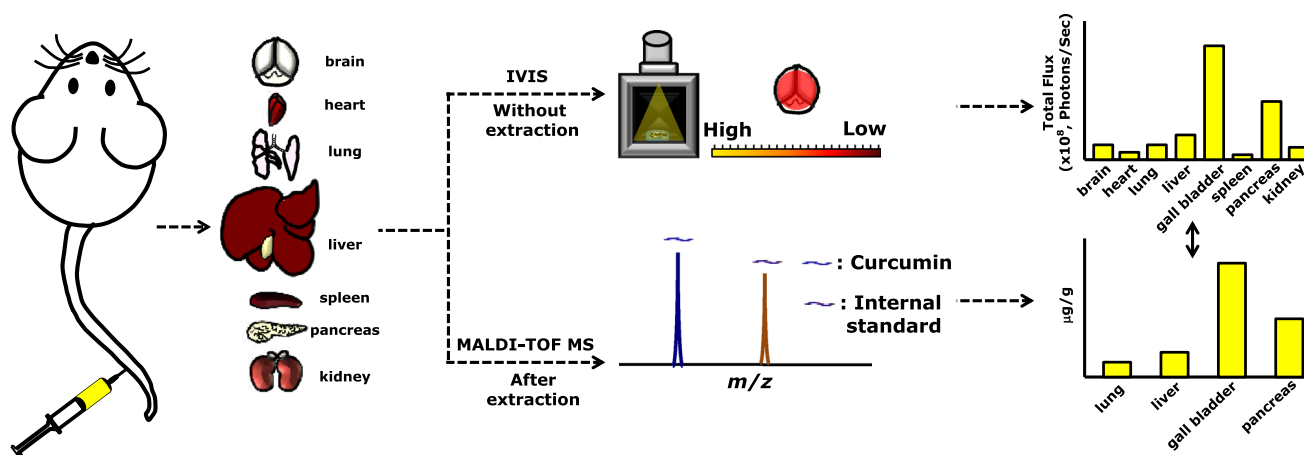
Fig. 1 Schematic illustration of in vivo administration of curcumin and subsequent analysis using combined imaging instrument and mass spectrometry to elucidate curcumin biodistribution

intravenous administration. After 1-h post-injection, each organ (the brain, heart, lung, liver, spleen, pancreas, and kidney) was isolated and visualized using the IVIS imaging instrument regardless of tissue extraction. Simultaneously, curcumin in each harvested organ was extracted and analyzed using MS, which provides quantitative information by using an internal standard. Comparative and complementary analysis of the resulting biodistribution data obtained from the in vivo optical imaging and MS is expected to provide more precise information regarding the in vivo fate of curcumin.

Figure 2A shows the optical fluorescence images of isolated organs after intravenous injection of curcumin at a dose of 25 mg/kg. Several tissues including the brain, lung, gall bladder, and pancreas showed obviously increased fluorescence signals after curcumin treatment, compared to the untreated samples. Only negligible signals were observed in the spleen and kidney. It is noteworthy that the untreated tissues such as the liver, gall bladder, and pancreas showed certain levels of fluorescent signals due to autofluorescence of the tissues. The fluorescence signals in each organ were also analyzed quantitatively as shown in Fig. 2B. The gall bladder and pancreas showed the highest fluorescence intensity of curcumin after injection. However, significant increase in the fluorescence signal was not observed in the liver following curcumin injection.

To quantify the curcumin contents of the isolated organs, curcumin was extracted using EA after homogenizing the organs. The dried extract of the organs was subsequently analyzed using MALDI-TOF MS in the presence of dimethylated curcumin as the internal standard. As shown in the representative mass spectra of the extracts from each organ (Fig. 2C), the curcumin and internal peaks can be clearly seen at m/z 369.13 and 397.16 $[M + H]^+$, respectively, while only a trace curcumin peak was

observed in the untreated tissues. The lungs, liver, gall-bladder, and pancreas showed significant curcumin contents, while other organs showed only trace or no signals for curcumin. Next, a calibration curve was constructed, and the peak intensities of curcumin and the internal standard were compared for the quantitative analysis of the curcumin contents in the organs (Fig. 2D).

Finally, we compared the quantitative results of the curcumin biodistributions obtained from the fluorescence imaging and mass analysis (Table 1). In both analyses, the gall bladder showed the highest curcumin content followed by the pancreas. The total flux extent of the brain, lung, liver, spleen, and kidney were 3.998 ± 0.058, 4.889 ± 0.213, 8.695 ± 8.096, 0.927 ± 0.879, and 2.790 ± 1.869 ($\times 10^8$ photons/s), respectively. Interestingly, similar total flux values for curcumin were observed in the brain and lungs. However, the curcumin content of the brain was negligible using the mass analysis in contrast to optical fluorescence imaging. The accumulated curcumin content of the lung was higher by ~ 20-fold than that of the brain was in the MS analysis, as shown in Table 1 right column. This result might be attributable to an insufficient extraction of curcumin from the brain using the current extraction process. In a previous study, the curcumin content of the lung was significantly higher than that of the brain was when curcumin was extracted and analyzed using HPLC (Song et al. 2011). Furthermore, the distribution of curcumin in each organ such as the kidney 1 h post intravenous injection was determined differently in previous studies (Song et al. 2011; Tsai et al. 2011). The discrepancies between the results of previous studies might be attributable to the susceptibility of curcumin to degradation during the extraction processes as well as different extraction efficiencies from the lung and brain using the same extraction protocol. In addition, the curcumin content
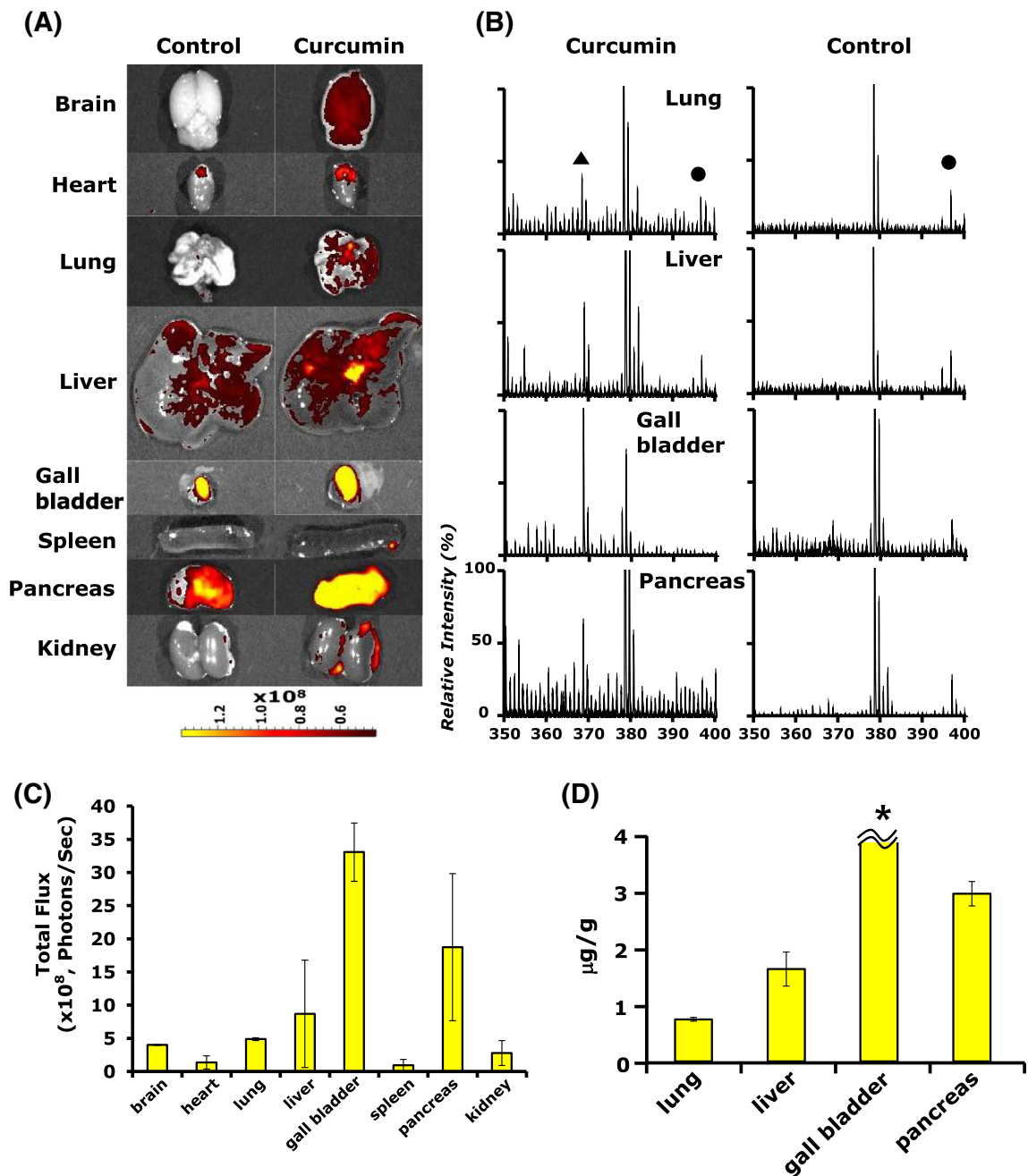
Fig. 2 (A) Visualization of fluorescence image (FI) of each organ after intravenous injection of ICR mice with curcumin. (B) Quantitative analysis of total flux in each organ using In Vivo Imaging System (IVIS) imaging program. Data are mean ± standard deviation (SD); $^{*}P < 0.05$ and $^{**}P < 0.001$; ns, not significant. (C) Representative mass spectra of extracts from each organ. *Filled triangle* curcumin and *Filled circle*, internal standard. (D) Quantitative analysis of curcumin in each organ obtained from (C)

of the liver was precisely determined using MS while ambiguous fluorescent images of the liver are evident in Fig. 2A due to autofluorescence of the liver tissue.

In this study, complementary analysis using optical fluorescence imaging and MS was performed for the precise determination of in vivo curcumin biodistribution after intravenous administration. The relative curcumin biodistribution in the heart, spleen, and kidney was similarly determined using optical fluorescence imaging and MS. However, significant accumulation of curcumin in the brain was only observed using fluorescence imaging without tissue extraction. The exact and reliable measurement of the curcumin accumulation in tissues with high autofluorescence such as the liver, gall bladder, and pancreas was determined using MS. Taken together, these results indicate that complementary analysis using optical

Table 1 Comparison of biodistribution of curcumin obtained from fluorescence imaging and mass analysis

Organs	IVIS (x10^8, Photons/Sec)	MS (μg/g)
Brain	3.998±0.058	0.037±0.002
Heart	1.370±0.999	n.d.
Lung	4.889±0.213	0.771±0.035
Liver	8.695±8.096	1.693±0.035
Gall bladder	33.073±4.397	>10
Spleen	0.927±0.879	0.037±0.012
Pancreas	18.741±11.092	3.075±0.225
Kidney	2.790±1.869	0.041±0.005

n.d. not determined

fluorescence imaging and MS allowed the precise determination of curcumin biodistribution in vivo. Therefore, this analytical strategy could be applied to a wide range of fluorescent polyphenols.

References

Anand P, Kunnumakkara AB, Newman RA, Aggarwal BB (2007) Bioavailability of curcumin: problems and promises. Mol Pharm 4(6):807–818

Choy G, O'Connor S, Diehn FE, Costouros N, Alexander HR, Choyke P, Libutti SK (2003) Comparison of noninvasive fluorescent and bioluminescent small animal optical imaging. Biotechniques 35(5):1022–1026

Kakkar V, Mishra AK, Chuttani K, Kaur IP (2013) Proof of concept studies to confirm the delivery of curcumin loaded solid lipid nanoparticles (C-SLNs) to brain. Int J Pharm 448(2):354–359

Kim MK, Jeong W, Kang J, Chong Y (2011) Significant enhancement in radical-scavenging activity of curcuminoids conferred by acetoxy substituent at the central methylene carbon. Bioorg Med Chem 19(12):3793–3800

Kim S, Oh HS, Yeo WS (2015) Analysis of alkanethiolates on gold with matrix-assisted laser desorption/ionization time-of-flight mass spectrometry. J Korean Soc Appl Biol Chem 58(1):1–8

Naksuriya O, Okonogi S, Schiffelers RM, Hennink WE (2014) Curcumin nanoformulations: a review of pharmaceutical properties and preclinical studies and clinical data related to cancer treatment. Biomaterials 35(10):3365–3383

Pan MH, Huang TM, Lin JK (1999) Biotransformation of curcumin through reduction and glucuronidation in mice. Drug Metab Dispos 27(4):486–494

Song ZM, Feng RL, Sun M, Guo CY, Gao Y, Li LB, Zhai GX (2011) Curcumin-loaded PLGA-PEG-PLGA triblock copolymeric micelles: preparation, pharmacokinetics and distribution in vivo. J Colloid Interface Sci 354(1):116–123

Tsai YM, Chien CF, Lin LC, Tsai TH (2011) Curcumin and its nanoformulation: the kinetics of tissue distribution and blood-brain barrier penetration. Int J Pharm 416(1):331–338

Zhang XL, Tian YL, Zhang C, Tian XY, Ross AW, Moir RD, Sun HB, Tanzi RE, Moore A, Ran CZ (2015) Near-infrared fluorescence molecular imaging of amyloid beta species and monitoring therapy in animal models of Alzheimer's disease. Proc Natl Acad Sci USA 112(31):9734–9739